7. Moreno, L. and Neretnieks, I., Flow and transport in fractured media: the importance of the flow-wetted surface for radionuclide migration. *J. Contam. Hydrol.*, 1993, **13**, 49–71.
8. Tsang, C. F., Tsang, Y. W. and Hale, F. V., Tracer transport in fractures: analysis of field data based on a variable-aperture channel model. *Water Resour. Res.*, 1991, **27**, 3095–3106.
9. Darcy, H., *Les Fontaines Publiques de la Ville de Dijon*, Dalmont, Paris, 1856.
10. Slichter, C. S., Theoretical investigations of the motion of ground waters. U.S. Geological Survey, 19th Annual Report. Part 2, 1899.
11. Kozeny, J., Uber kapillare Leitung der Wasser in Boden, Sitzungsber. *Akad. Wiss. Wien*., 1927, **136**, 271–306.
12. Carman, P. C., Permeability of saturated sands, soils and clays. *J. Agric. Sci*., 1939, **29**, 262–273.

Received 19 June 2015; revised accepted 4 November 2015

doi: 10.18520/cs/v110/i4/695-701

Delineation of groundwater saturation indicators and their distributions in the complex argillaceous geological units of Ezza north local government area of Ebonyi state, Nigeria

Daniel N. Obiora[1,]*, Johnson C. Ibuot[1], Nyakno J. George[2] and Solomon U. Offiah[3]

[1]Department of Physics and Astronomy, University of Nigeria, Nsukka, Enugu State, Nigeria
[2]Department of Physics, Akwa Ibom State University, Ikot Akpaden, Uyo, Akwa Ibom State, Nigeria
[3]National Centre for Energy Research and Development, University of Nigeria, Nsukka, Enugu State, Nigeria

Twelve vertical electrical soundings (VES) employing Schlumberger electrode configuration were carried out in parts of Ezza north local government area of Ebonyi state, Nigeria, where extraction of potable groundwater has posed challenges to the dwellers of the area who are currently relying on surface water sources and some scattered seasonal open wells that cause health problems. The present study was undertaken to determine the hydrogeological characteristics, indicators that predict groundwater potential of the study area. The study indicates that the aquifer resistivity ranges between 12 and 504 Ωm with an average value of 95.42 Ωm. Water resistivity ranges between 9.6 and 73.0 Ωm with an average of 26.34 Ωm. The aquifer thickness ranges from 34.1 to 214.7 m with an average of 71.97 m. Also, the formation factor varies between 1.25 and 6.9 with an average of 2.76. Porosity ranges between 5.34% and 29.47% with an average of 15.91%. Similarly, hydraulic conductivity ranges from 1.1645 to 38.0491 m/day, the average being 12.8312 m/day, and $K\sigma$ values range between 0.0023 and 3.1695 S/day with a mean value of 0.6273 S/day. Using surfer software package, contour distributions of geo-hydrodynamic properties were generated which show the distribution of the aquifer parameters in the study area. The distributions of these properties reflect the regions with high and low potential groundwater in the area. The diagnostic models and the inherent and intrinsic constants can be employed in quantitative prediction of groundwater potential in the adjoining regions of the study area which show similar hydrogeological properties.

Keywords: Argillaceous geological units, groundwater potential, hydrogeological properties, vertical electrical sounding.

GROUNDWATER is the major source of water supply needed by humans for industrial, agricultural and domestic purposes. The natural quality is usually good, and it is resistant to even prolonged droughts[1]. Groundwater occurrence, storage and flow in a hard-rock terrain are controlled by the geology, geomorphology, divide and structure. Groundwater is usually contained within the weathered and tectonically induced geological features, fractured/fissured, sheared or jointed/faulted columns of rock units. These rock units are altered by geological processes. This alteration causes reduction in resistivity at depth of burial and a noticeable increase in secondary porosity, coefficient of permeability and permeability which are the major hydrodynamic properties[2] that serve as indicators and dependent factors that decide the distribution of units for groundwater accumulation, discharge and exploitation[3]. Within the last decade, hydrogeological information has been increasingly complemented with surface geophysical information that allows for more accurate images of aquifer systems[4]. Electrical resistivity method is versatile and economical for delineating the locations of productive aquifer sites and apparent thickness of the weathered zone, which is useful in siting boreholes in dense rocks. Layers in hard rocks characterized by thick fractures have high secondary porosity/permeability that connotes prolific geological units. The knowledge of electrical geophysical survey as an example can be used to assess aquifer potential of an area, thus, reducing the cases of failed boreholes. A detailed qualitative knowledge of water transmitting properties of an aquifer is crucial for successful groundwater development and management practices in an area. The efforts of government and non-governmental agencies in providing safe drinking water to some communities have recorded great successes, and have aided in not only solving the water scarcity problem, but also curbing the outbreaks of some waterborne diseases like cholera, diarrhoea, typhoid, guinea worm, etc. To avoid the cases of failure of some boreholes in the study area, there is need for a systematic study in order to delineate the potential groundwater

*For correspondence. (e-mail: daniel.obiora@unn.edu.ng)

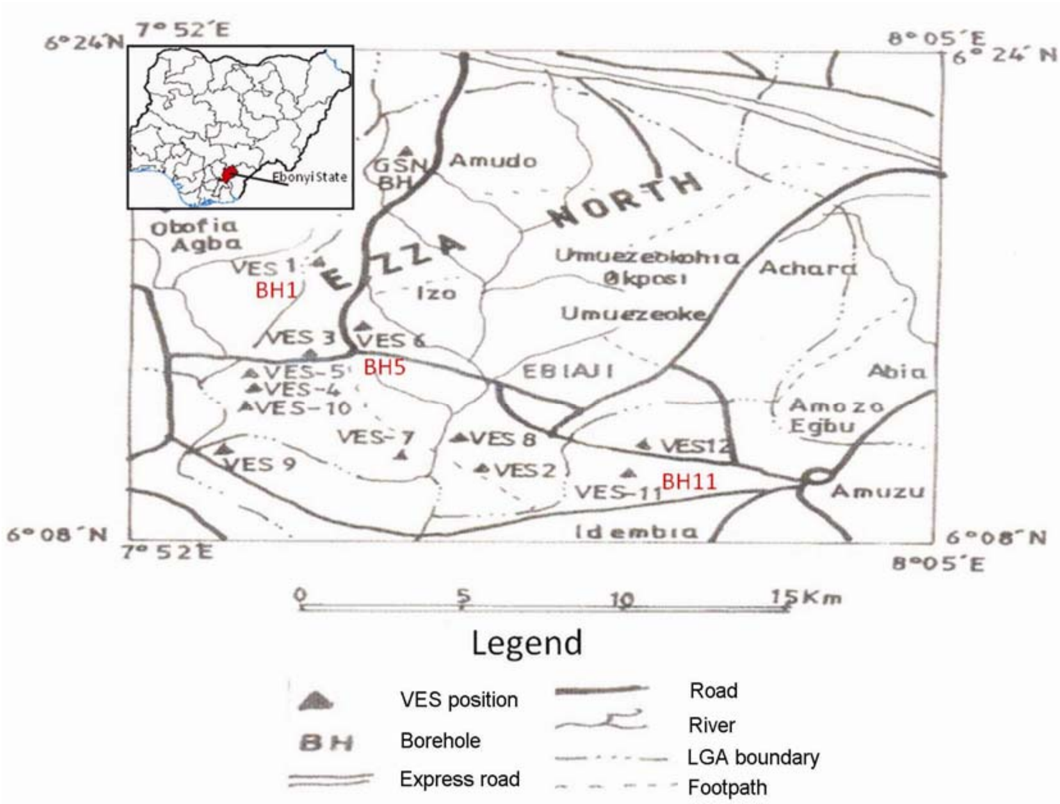

Figure 1. Schematic map showing the study area, vertical electrical sounding (VES) locations and boreholes used as control in the study.

indicators[5,6]. The search for groundwater is faced with several uncertainties. Porosity and permeability of the host rocks are two major determinants of the availability, quantity and exploitability of groundwater. Factors that determine the porosity of rocks include cracks, fractures, faults and vesicles in volcanic rocks.

The major objective of the present study is to delineate the subsurface hydrogeological characteristics and groundwater potential of the area, in order to ease the problem of water scarcity and improve the living standard of the people through accessibility to potable water. The diagnostic models can be useful in estimating parameters that furnish information about the quality and quantity of groundwater in the study area.

The study area lies on the southeastern part of Nigeria between lat. 06°08′N–06°17′N and long. 07°52′E–07°00′E (Figure 1). The area covers about 246 sq. km and lies in the southeastern part of Ebonyi state Nigeria. The study area belongs to the Asu River Group shales. The sediments of the Asu River Group which were formed during the Albian had folded into open northeast trend known as Abakaliki Anticlinorium[7]. The Asu River Group is overlain by a succession of shale, siltstone and sandstone, with shallow marine fauna and is estimated to have a maximum thickness of about 200 m. There are some mineral intrusions which may have contributed to its numerous fractures. The geological survey around the area reveals that the location is part of the Ebonyi Formation. This Formation overlies the Abakaliki siltstone and sandstone previously referred to in the literature as the Unknown 'Formation'[7]. It is now referred to as Ebonyi Formation[8]. The Formation underlies a gentle undulating terrain in Ntezi-Ezamgbo area southward of Amagu–Agba. The Ebonyi River and its tributaries (Akaduru, Nramura and Isumutu) form the major drainage system in the area. The Formation is divided into three units from top to bottom: the upper siltstone–shale sequence is exposed at Amagu–Agba village. It consists essentially of rapidly alternating siltstone and silty shale with occasional thin sandstone beds. The middle limestone–siltstone sequence unit outcrops at a quarry, 2 km from Ekemoha–Agba road junction. It consists of minor sandstone, siltstone, limestone and shale, and the lower mudstone–shale sequence exposed at Umuezeoke, along the drainage cut by River Akaduru. This sequence is greyish, occasionally flesh-coloured and bedded with dark micaceous steaks. The study area has an elevation between 57 and 89 m amsl. Marshy conditions of lower elevation that also exist within the area are noted for rice production. Most of the streams existing in the area are seasonal. The seasonal rivers which are active during the rainy season have the major drainage, the Ebonyi River, which flows to the Cross River, some distance to the south near Afikpo. The mudstones are highly weathered on the top.

Significant groundwater is only found where the mudstone and shale are highly fractured.

The vertical electrical sounding (VES) data were acquired using the OHMEGA SAS1000 Terrameter. A total of 12 geoelectric soundings were obtained employing Schlumberger array with half current electrode separation (*AB*/2) of 150 m and half potential electrode separation (*MN*/2) of 15 m. The apparent resistivity (ρ_a) and thickness (h) are the two fundamental parameters which define the geoelectric layer. The bulk electrical resistivity values of geologic formations are related to the subsurface rock properties like the type of rock and soil, porosity, extent of saturation, nature of the saturating fluid and diagenetic cementation factors[9–12]. The bulk electrical resistivity (ρ_b) is related to the electrical resistivity of water (ρ_w) and porosity (ϕ) by the relation[9]

$$\rho_b = a\rho_w\phi^{-m}, \tag{1}$$

where a is an empirical constant while m is the cementation factor. Water resistivity (ρ_w) which affects the resistivity of a rock formation is related to formation factor (F) and formation bulk resistivity (ρ_b) by the relation[9]

$$\rho_b = F\rho_w, \tag{2}$$

or

$$F = \frac{\rho_b}{\rho_w}. \tag{3}$$

Hydrological and hydrogeological problems, such as characterization of aquifer formation, mapping of saturated aquifer horizons and groundwater contamination studies have been undertaken using the resistivity method[5,13–16]. According to Niwas and Singhal[17], the analytical relationship between aquifer transmissivity (T), hydraulic conductivity (K) and aquifer thickness (h) is given by

$$T = Kh. \tag{4}$$

According to Heigold *et al.*[18]

$$K = 386.40\,\rho_b^{-0.93283}, \tag{5}$$

where ρ_b is the resistivity of aquifer. Equation (5) was used to estimate the hydraulic conductivity K (m/day). The aquifer bulk conductivity $\sigma(1/\rho_b)$ was calculated for each VES station and multiplied with the estimated hydraulic conductivity obtained through the use of diagnostic constants in eq. (5) to determine the values of $K\sigma$ (Table 1). The $K\sigma$ values were assumed to remain fairly constant in areas of similar geologic setting and water quality[17,19].

The computation of apparent resistivity from the measured resistance was done using the expression in eq. (6)

$$\rho_a = \pi\left[\frac{(AB/2)^2 - (MN/2)^2}{MN}\right]R_a, \tag{6}$$

where *AB* is the distance between the two current electrodes, *MN* the distance between the potential electrodes, and R_a is the apparent electrical resistance measured from the equipment. Equation (6) can be reduced to

$$\rho_a = GR_a, \tag{7}$$

where G is the geometric factor given by

$$G = \pi\left[\frac{(AB/2)^2 - (MN/2)^2}{MN}\right].$$

The manual procedure was followed by plotting the computed apparent resistivity data on a bi-logarithmic graph and the curves generated were smoothened to remove the effects of lateral inhomogeneities and other forms of noisy signature[20]. The smoothed curves were quantitatively interpreted in terms of true resistivity and thickness by a conventional manual curve matching procedure using master curves and auxiliary charts[21]. The RESOUND software package was later used to improve the manually interpreted data and the results were transformed to their equivalent geoelectrical models. The data for the estimated model were generated with the software program and the result was compared with the measured counterpart. The software works iteratively by calculating at the end of each step updated parameters of the model and also the extent of fit between the calculated and observed data using the root mean square error (RMSE) technique in which 6% was preset as the maximum acceptable value[22]. In Figure 2, typical geologic models obtained are shown along with their correlations with nearby boreholes.

Both manual and computer modelling techniques were employed in the reduction of VES data to their equivalent 1D geological models. The manual procedure involves plotting the computed apparent resistivities on bi-logarithmic graphs and where necessary, smoothening the curves generated in order to remove the effects of lateral heterogeneities and other forms of noisy signature. This was performed by averaging the two readings at the crossover points, or deleting any outlier at these points that did not conform to the dominant trend of the curve. The data which stood out as outliers in the prevalent curve trend were also deleted; these could have caused increase in RMSE during the modelling phase of the study. Preliminary interpretation of the smoothed curves was made using the traditional partial curve matching technique to

Table 1. Results of aquifer electrical and hydraulic parameters

VES	Longitude (°)	Latitude (°)	ρ_b (Ωm)	ρ_w (Ωm)	*h*(m)	*F*	ϕ (%)	*K* (m/day)	$K\sigma$(S/day)	*T* (m^2/day)
Adiagu-Oguji Nwudor	7.9183E	6.9183N	51	20.8	34.1	2.45	15.03	9.8665	0.1933	336.45
Ekka Town Hall, Azugwu	7.9500E	6.1800N	24	13.6	46.4	1.77	20.82	19.9313	0.8311	924.81
Nkomoro-Omuzor Ogbo Ojiovu	7.9261E	6.2367N	19	11.4	49.4	1.67	22.06	24.7843	1.3037	1224.34
Ndiegu-Ogboji-Ukwu, Akpara	7.0844E	6.2222N	95	32.6	214.7	2.91	12.66	5.5228	0.058	1185.75
Umundiegu-Ohaike	7.9022E	6.2339N	23	12.9	71.3	1.78	20.69	20.7385	0.9021	1478.66
Udenyi-Azuakparata	7.9261E	6.2564N	50	20.3	48.4	2.46	14.98	10.0505	0.201	486.44
Inyere-Ngangbo Nwakpa Umobi	7.9247E	6.1806N	93	31.5	63.9	2.95	12.49	5.6335	0.0608	359.98
Ogboji-Eguo-Ugwu	7.9539E	6.1833N	504	73.0	77	6.9	5.34	1.1645	0.0023	89.67
Ohaccara-Ndiegu-Ohaccara	7.8850E	6.1953N	120	36.4	52.5	3.3	11.16	4.4415	0.0369	233.18
Ndiegu Ekka-Onunwode, Ndiegu	7.8906E	6.2072N	64	24.3	84.7	2.63	14.01	7.9832	0.1245	676.18
Ekka Integrated Primary School, Ekka	8.0161E	6.1706N	12	9.6	55.2	1.25	29.47	38.0491	3.1695	2100.31
Ohaugo Primary School, Ekka	7.9847E	6.1739N	90	29.7	66	3.03	12.16	5.8085	0.6447	383.36
Average			95.42	26.34	71.97	2.76	15.91	12.8312	0.6273	71.97

estimate primary layer parameters. Computer-based VES modelling software called RESOUND, which can perform automated approximation of the initial resistivity model from the observed data, was later used to improve upon the preliminary interpreted results using the inversion technique. The software works iteratively by computing at the end of each step, updated parameters and the extent of fit between the calculated and the observed data. The RMSE technique in which 6% was preset as the maximum acceptable value was used in assessing the extent of fit. Representative VES curves 1, 5 and 11 in Figure 2 show good correlations between the nearby borehole lithologies and the interpreted VES results. The resistivity, depth and thickness were estimated as shown in Figure 2. Some correlations were observed between the borehole lithology logs and the inverted results. The VES curves and their associated data at stations 1, 5 and 11 have been typically drawn in Figure 2 in order to show the curve variation within the geological province under study.

Table 1 also shows the results of interpretation of aquifer VES data. The 12 stations with the values of aquifer resistivity (ρ_b), aquifer water resistivity (ρ_w), aquifer thickness (*h*), formation factor (*F*), porosity (ϕ), hydraulic conductivity (*K*) and $K\sigma$ (hydraulic conductivity × aquifer bulk conductivity); referred to as groundwater saturation diagnostic indicators are shown in the table. Apart from bulk resistivity and water resistivity, which are calculated and measured using analysis of geophysical data and water samples respectively, the other parameters were calculated using their respective equations mentioned above. These values were contoured using Surfer-10 Subroutine program, and plotted as graphs between two parameters using Microsoft Excel, 2007.

The aquifer bulk resistivity has a range 12–504 Ωm and an average value of 95.42 Ωm. The resulting contour map of resistivity (Figure 3) has higher values at the eastern and western regions of the mapped area. It can also be inferred that the study area is dominated by shale and sandstone. Ogboji-Ekwu-ukwu with the highest resistivity value will be a zone with the highest yielding well. The inferred contour map of water resistivity (Figure 4) shows on the average, a decrease in resistivity from west to east of the mapped area. The segments with low resistivity indicate the presence of abundant argillaceous materials which could impede groundwater saturation and flow. Formation factor (*F*) estimated from the ratio of ρ_b to ρ_w ranges from 1.25 to 6.9 with an average of 2.76. The contour map of *F* (Figure 5) shows lower values which is an evidence of high water electrical resistivity or low electrical conductivity. The lower *F* values sandwiched between the eastern and western parts of the mapped area indicate that the water in the eastern and western extremities is likely to be influenced by argillaceous materials of clay or shale.

Aquifer thickness has a range 34.1–214.7 m. The mean average thickness of 71.97 m in the study area is indicative of prolific groundwater potential. The contour map of aquifer thickness (Figure 6) shows a decrease from east to west of the study area. This is a clear indication of high potential groundwater in the eastern sector (near Ndiegu-ogboji-ukwu Akpor with a value of 214.7 m) than the western sector. It can be concluded that the eastern region is likely to have higher transmissivity than the western region of the mapped area. The variations in the thickness of aquifers in the study area are due to the variation of lithologic composition of the subsurface which is characterized by the high ranges of resistivity.

The porosity (ϕ), which varies inversely with *F* as shown in Figure 7, ranges from 5.34% to 29.47% with an average value of 15.91%. From the figure, it can be seen that ϕ decreases on the average, from east to west of the mapped area. This is an indication of the presence of more communicating pores east of the study area than in the west. Invariably, the western region of the study area may likely have dead-end pores, thereby impeding groundwater flow.

Again, the hydraulic conductivity (*K*), which varies between 1.1645 and 38.0491 m/day with an average of 12.8312 m/day, shows similar distribution as porosity

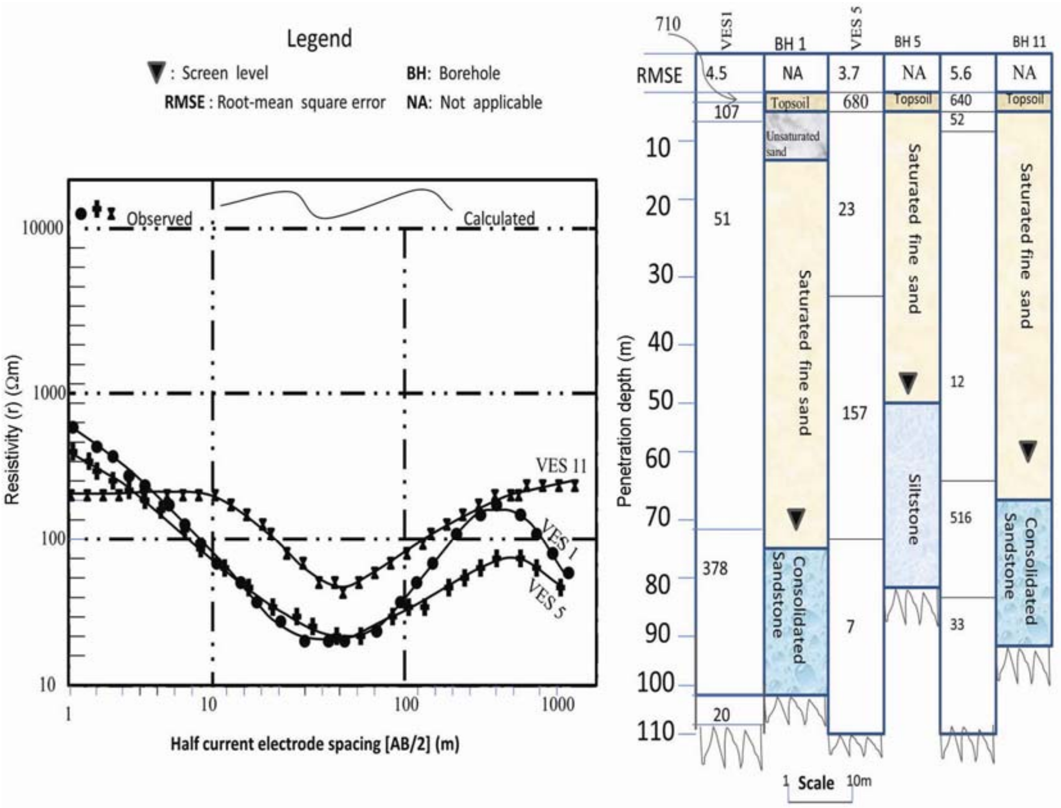

Figure 2. Samples of 1D-derived modelled VES curves correlating with nearby borehole lithologs in the study area.

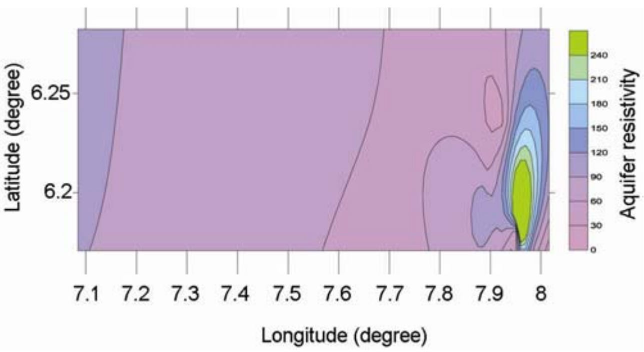

Figure 3. Contour map showing distribution of aquifer bulk resistivity in the study area.

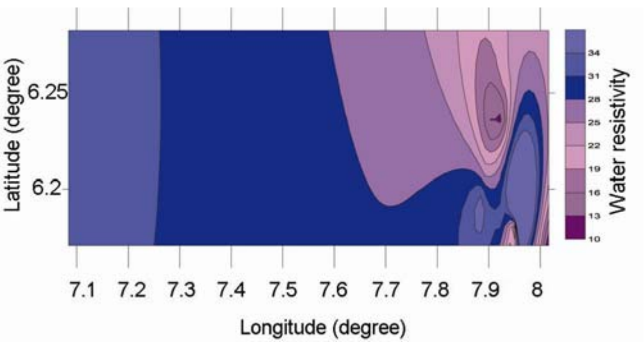

Figure 4. Contour map showing variation of water resistivity in the study area.

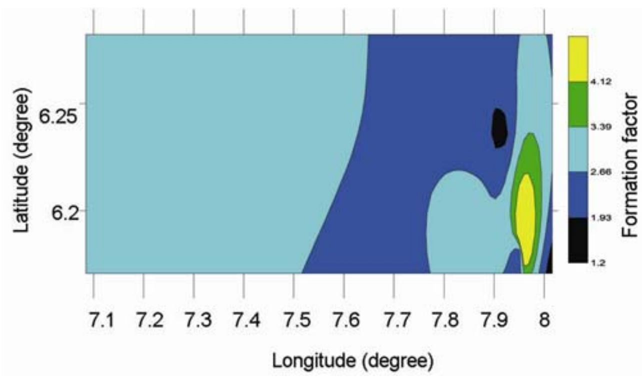

Figure 5. Contour map showing the variation of formation factor in the study area.

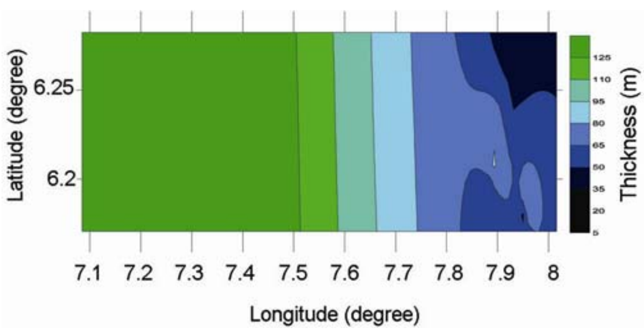

Figure 6. Contour map showing the distribution of aquifer thickness in the study area.

(Figure 8). The extant seemingly high variations in the value of K, are symptomatic of the inhomogeneity of facies change and variation in grain size[2]. In analogy with porosity and coefficient of permeability (K), $K\sigma$ decreases from the eastern region of the study area to the western region (Figure 9). The $K\sigma$ values range from 0.0023 to 3.1695 S/day with a mean value of 0.6273 S/day. This indicates that highly conductive ions will be found in the area with low resistivity which extends from southeast to the western part of the study area. The area with reasonably high $K\sigma$ values indicates zones with protective hydrological units believed to be characterized by freshwater.

Figure 10 indicates the diagnostic models showing aquifer resistivity (ρ_b) versus water resistivity (ρ_w). From the graph, a positive correlation (R_c = 0.9935) is obtained between the two variables

$$\rho_b = 0.2554\,\rho_w^{1.7348}. \quad (8)$$

The power law in eq. (8) gives a direct relationship between bulk water resistivity and pore-water resistivity.

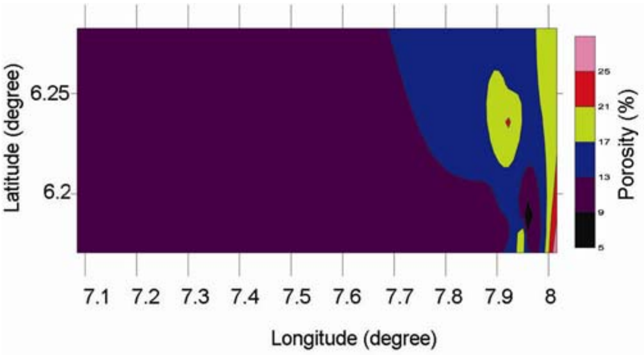

Figure 7. Contour map of porosity distribution in the study area.

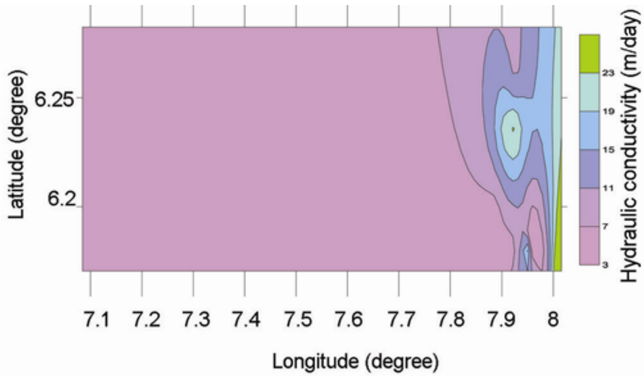

Figure 8. Contour map of hydraulic conductivity showing its distribution in the study area.

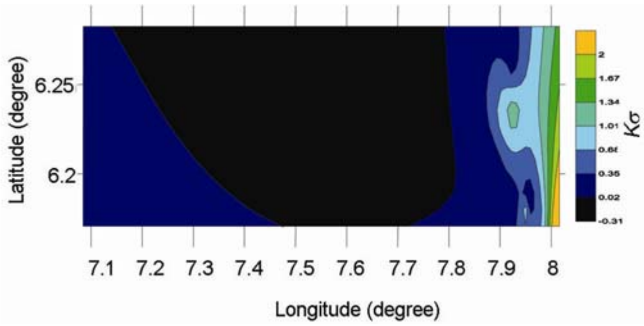

Figure 9. Contour map showing the distribution of $K\sigma$ in the study area.

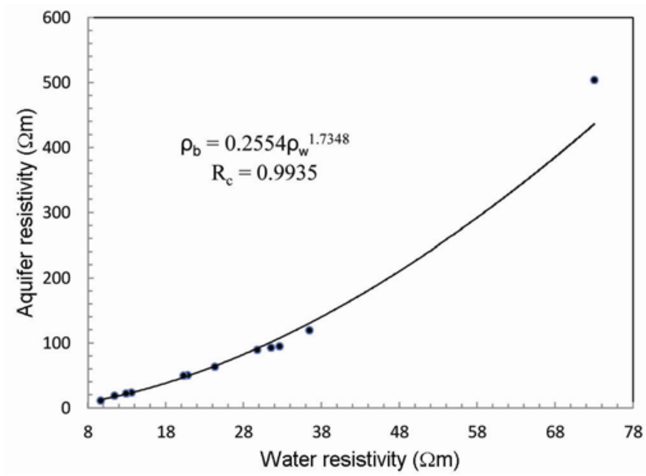

Figure 10. A graph of aquifer bulk resistivity against water resistivity.

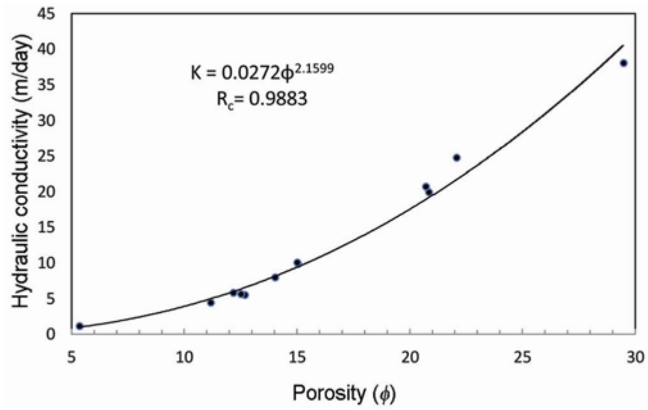

Figure 11. A graph of hydraulic conductivity against porosity.

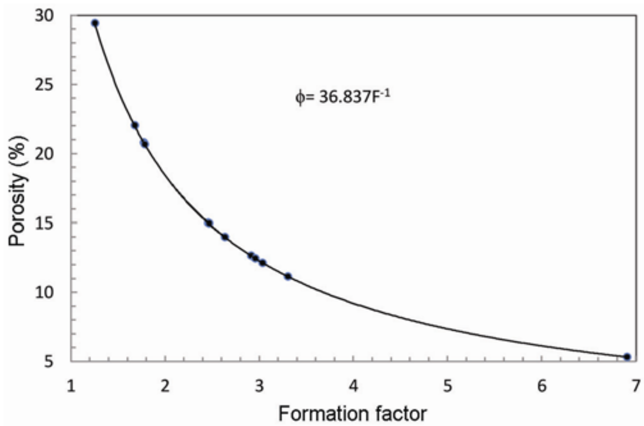

Figure 12. A graph of porosity against formation factor.

The diagnostic constants can be used to estimate hydrodynamic properties of the other region of the cuesta.

The graph of hydraulic conductivity (K) versus porosity (ϕ) also shows a positive correlation ($R_c = 0.9883$) and a diagnostic relation given in Figure 11 is expressed in eq. (9) as

$$K = 0.0272\phi^{2.1599}. \quad (9)$$

The model with increase in hydraulic conductivity as porosity increases can be used to estimate with certainty the indices of contamination, groundwater abstraction rate and flow direction. These diagnostic models can be used to demystify the complex nature of hydrogeological and geoelectrical compositions of the Ezza north local government area of Ebonyi state.

Porosity as transmitting property plays a vital role in groundwater availability as its value in a medium determines whether an aquifer is active or not. Porosity, which increases as formation factor decreases (Figure 12) due to increase in water resistivity in hydrogeological units, is one of the indicators of groundwater saturation or reserve in a geological unit. The values determined from the work indicate that the area has a high potential when the screen is placed in the sizable saturated unit. The study area shows highly variable depth and thickness of saturated geological units according to the geological lithostratigraphic logs or geologic sequence and the inferred VES data. The highly correlated diagnostic expression in eq. (10) can be used in the study area to estimate the degree of saturation of the pore spaces and their inter connectedness.

$$\phi = 36.837F^{-1}. \quad (10)$$

The enhancement of knowledge regarding hydrogeology in Ezza using VES will help in groundwater development and management. Twelve VES have been used to evaluate the subsurface hydrogeological conditions of the study area. The aquifer resistivity values obtained from different locations are indicative of the formation present. From the interpretation, the hydraulic behaviour of the groundwater flow system and potential is affected by the presence of argillaceous materials. Most of the accessible aquifers in this study are porous and highly productive, but characterized by low resistivities. This behaviour is suspected to be due to the nature of the saturating fluid which is affected by biochemical, physical and geological controls. Highly and poorly conductive zones in the study area have also been delineated. The contour maps show the lateral and vertical variations of resistivity, thickness, porosity, formation factor, hydraulic conductivity and $K\sigma$ value within the hydrogeological units. These parameters calculated from interpreted resistivity soundings emphasize the contribution of the geophysical methods in the determination of aquifer hydraulic parameters and the potential of potable water in the area. Therefore, their distributions are good indices of groundwater saturation indicators. These parameters estimated in this preliminary study would be useful in modelling groundwater contamination in the study area where potable water is highly sought after.

1. Adetola, B. A. and Igbedi, A. O., The use of electrical resistivity survey in location of aquifers: a case study in Agbede, South Western Nigeria. *J. Niger. Assoc. Hydrogeol*., 2000, **11**, 7–13.
2. George, N. J., Emah, J. B. and Ekong, U. N., Geohydrodynamic properties of hydrogeological units in parts of Niger Delta, southern Nigeria. *J. Afr. Earth Sci*., 2015, **105**, 55–63.
3. Mohammed, M. Z., Ogunribido, T. H. T. and Funmilayo, A. T., Electrical resistivity sounding for subsurface delineation and evaluation of groundwater potential of Araromi Akungba-Akoko Ondo State Southwestern Nigeria. *J. Environ. Earth Sci*., 2012, **2**(7), 29–40.
4. Ibuot, J. C., Akpabio, G. T. and George, N. J., A survey of the repository of groundwater potential and distribution using geoelectrical resistivity method in Itu Local Government Area, Akwa Ibom State, southern Nigeria. *Central Eur. J. Geosci*., 2013, **5**(4), 538–547.
5. Akpan, A. E., Ugbaja, A. N. and George, N. J., Integrated geophysical, geochemical and hydrogeological investigation of shallow groundwater resources in parts of the Ikom-Mamfe Embayment and the adjoining areas in Cross River State, Nigeria. *Environ. Earth Sci*., 2013, **70**(3), 1435–1456.
6. Coker, J. O., Makinde, V. and Olowofela, J. A., Geophysical investigation of groundwater potentials of Oke-Badan Estate, Ibadan, Southwestern. Nigeria. In Proceedings of 3rd International Conference on Science and National Development, University of Agriculture, Abeokuta, Nigeria, 2009, pp. 119–123.
7. Reyment, R. A., *Aspect of Geology of Nigeria*, University of Ibadan Press, Ibadan, Nigeria, 1965.
8. Agumanu, A. E., The Abakiliki and the Ebonyi Formations: subdivisions of the Albian Asu River Group in the Southern Benue Trough, Nigeria. *Bull. Geol. Surv. Niger*., 1990, **9**, 195–206.
9. Archie, G. E., The electrical resistivity log as an aid in determining some reservoir characteristics. *Trans. Am. Inst. Min. Metall. Pet. Eng*., 1942, **146**, 54–62.
10. Smith, R. C. and Sjogren, D. B., An evaluation of electrical resistivity imaging (ERI) in Quaternary sediments, Southern Alberta, Canada. *Geosphere*, 2006, **2**(6), 287–298.
11. Batayne, A. T., A hydrogeophysical model of the relationship between geoelectric and hydraulic parameters, Central Jordan. *J. Water Res. Prot*., 2009, **1**, 400–407.
12. Obinawu, V. I., George, N. J. and Udofia, K. M., Estimation of aquifer hydraulic conductivity and effective porosity distributions using laboratory measurements on core samples in the Niger Delta. *Int. Rev. Phys*., 2011, **5**(1), 19–24.
13. Singh, U. K., Das, R. K. and Hodlur, G. K., Significance of Dar–Zarrouk parameters in the exploration of quality affected coastal aquifer systems. *Environ. Geol*., 2004, **45**, 696–702.
14. Ogilvy, R. D. *et al.*, Automated monitoring of coastal aquifers with electrical resistivity tomography. *Near Surf. Geophys*., 2009, **7**, 367–375.
15. Gemail, K. S., El-Shishtawy, A. M., El-Alfy, M., Ghoneim, M. F. and Abd El-Bary, M. H., Assessment of aquifer vulnerability to industrial waste water using resistivity measurements – a case study, along El-Gharbyia main drain, Nile Delta, Egypt. *J. Appl. Geophys*., 2011, **75**, 140–150.
16. George, N. J., Ubom, A. I. and Ibanga, J. I., Integrated approach to investigate the effect of leachate on groundwater around the Ikot Ekpene Dumpsite in Akwa Ibom State, Southeastern Nigeria. *Int. J. Geophys*., 2014, **2014**, 1–12.
17. Niwas, S. and Singhal, D. C., Estimation of aquifer transmissivity from Dar Zarrouk parameters in porous media. *Hydrology*, 1981, **50**, 393–399.

18. Heigold, P. C., Gilkeson, R. H., Cartwright, K. and Reed, P. C., Aquifer transmissivity from surficial electrical methods. *Ground Water*, 1979, **17**(4), 338–345.
19. George, N. J., Obianwu, V. I. and Obot, I. B., Estimation of groundwater reserve in unconfined frequently exploited depth of aquifer using a combined surficial geophysical and laboratory techniques in the Niger Delta, South–South, Nigeria. *Adv. Appl. Sci. Res.*, 2011, **2**(1), 163–177.
20. Chakravarthi, V., Shankar, G. B. K., Muralidharan, D., Harinarayana, T. and Sundararajan, N., An integrated geophysical approach for imaging sub-basalt sedimentary basins: case study of Jam River Basin, India. *Geophysics*, 2007, **72**(6), 141–147.
21. Orellana, E. and Mooney, H., *Master Tables and Curves for VES over Layered Structures*, Interciencia, Madrid, Spain, 1966.
22. George, N. J., Akpan, A. E. and Obot, I. B., Resistivity study of shallow aquifer in parts of southern Ukanafun Local government area, Akwa Ibom State. *E-J. Chem.*, 2010, **7**(3), 693–700.

ACKNOWLEDGEMENTS. We thank Dr J. U. Chukudebelu and Prof. F. N. Okeke (Department of Physics and Astronomy, University of Nigeria, Nsukka) for encouragement and support. We also thank editor and the anonymous reviewers for their critical inputs and suggestions that helped improve the manuscript.

Received 17 February 2015; revised accepted 30 November 2015

doi: 10.18520/cs/v110/i4/701-708

Haematological and immunological response of *Achyranthes aspera* leaf and root extracts in arsenic-intoxicated female mice (*Mus musculus*)

Veena Sharma* and Rashmi Singh

Department of Bioscience and Biotechnology, Banasthali University, P.O. Banasthali 304 022, India

To evaluate therapeutic efficacy of *Achyranthes aspera* against arsenic toxicity, mice were given aqueous root and leaf extracts at both low and high doses (100 and 200 mg/kg body wt) after being intoxicated with sodium arsenate (0.1 mg/kg body wt). Significant alterations ($P < 0.05, 0.001$) were seen in various haematological parameters, Ig level, macrophage yield, viability, phagocytic index and progesterone level. Results clearly depict that both *A. aspera* extracts significantly restore the unbalanced level up to the normal. This study shows the protective efficacy of *A. aspera* on altered haematological and immunological system. It is possible that future work on drug formulation may use this plant as a source.

Keywords: *Achyranthes aspera*, arsenic toxicity, haematological alterations, mice immune system.

ARSENIC (As), is present in various forms in soils, pesticides, groundwater, drinking water, rocks and fossil fuels[1]. Presently, due to enhanced human activities like mining, smelting, coal combustion, etc., the level of arsenic has crossed its permissible limit and comes in contact with humans via various routes – inhalation, ingestion and dermal absorption. Inorganic As reacts with –SH group of cell proteins and inhibits various oxidative processes, thus leading to various health problems[2–4] like tissue hypoxia, cell damage, hepatic and central nervous system damage[5–8]. To combat As toxicity, a range of therapies are available that are based on chelation of As from the body via various synthetic agents that lead to severe side effects in the body. So, there is a need to develop a potent herbal drug that has fewer side effects and is more target specific.

Achyranthes aspera (family Amaranthaceae), a perennial stiff erect herb has cosmopolitan distribution. This plant is traditionally used in the treatment of various diseases like odontalogic, rheumatism, bronchitis, skin diseases, rabies[9], fever, dysentery and diabetes. The plant also works as an antiviral, anticoagulant, antihypertensive, diuretic, aphrodisiac, antifertility, antispasmodic and antitumour[10–12]. It has been reported that the leaf and root parts of *A. aspera* contain ecdysterone (phytoecdysone), oleanolic acid and other important bioactive constituents like flavonoids, saponins, alkaloids, glycosides, etc.[13]. Hence, recognizing the toxic effects of arsenic and the therapeutic efficacy of *A. aspera*, the present study was designed to evaluate the haematological obliterations and immune-modulating effect of *A. aspera* in sodium arsenate-intoxicated mice.

All chemicals used in the study were of analytical grade and were purchased from reliable firms (Sigma-Aldrich, SRL, Merck-Millipore, RanBaxy and HiMedia). Sodium arsenate, the experimental compound, was purchased from HiMedia, India.

A. aspera was collected from the roadside at the Banasthali University Campus, Rajasthan, India and was taxonomically identified by a botanist of Krishi Vigyan Kendra, Banasthali University. Root and leaf parts were separated from the whole plant, cleaned, shade-dried and powdered. Aqueous extracts of both parts were prepared by simple maceration method. The filtrates were concentrated under reduced pressure in a rotary evaporator (Heidolph Incarp Instruments Pvt Ltd, Germany) and stored at room temperature in desiccators for further analysis.

Female Swiss albino mice (weighing 20–30 g) were obtained from Haryana Agricultural University, Hissar, India for experimental purpose. The Animal Ethical Committee of Banasthali University approved the experimental protocol. All animals were housed in polypropylene cages under well-maintained temperature (25 ± 3°C) with 12 h alternating light and dark cycle. Mice were provided nutritionally adequate pelleted chow diet (Ashirwad Pvt Ltd, India) and drinking water *ad libitum* throughout the study.

*For correspondence. (e-mail: drvshs@gmail.com)